

# Liver fibrosis processing, multiclassification, and diagnosis based on hybrid machine learning approaches

Zainab Sattar Jabbar<sup>1</sup>, Auns Qusai Al-Neami<sup>1</sup>, Ahmed A Khawwam<sup>2</sup>, Sufian Munther Salih<sup>1</sup>

<sup>1</sup>Department of Biomedical Engineering, College of Engineering, Al-Nahrain University, Baghdad, Iraq

<sup>2</sup>Faculty of Dentistry, Al-Kufa University, Najaf, Iraq

## Article Info

### Article history:

Received Jun 5, 2022

Revised Oct 7, 2022

Accepted Oct 11, 2022

### Keywords:

Convolutional neural network

Deep learning

Liver fibrosis

Shear wave elastography

## ABSTRACT

The cirrhosis and cirrhosis-related problems are connected to the degree of fibrosis in the liver. The purpose of this paper is to propose an automated method for identifying liver fibrosis using ultrasound shear wave elastography (700) images that is based on a hybrid machine learning approach using a convolutional neural network (CNN) with two types of classifier (SoftMax and support vector machine (SVM)). The dataset gathered from hospitals is used in the training and testing phases of the model. The objective is to develop a hybrid machine learning model that can classify images based on their stage of fibrosis. The suggested system comprises three stages. The first is the preprocessing step, which starts with contour detection and continues with the "contrast limited adaptive histogram equalization (CLAHE)" technique to show the properties of liver tissue. In the second step, the CNN algorithm was utilized, which was based on several images to extract deep features and identify shear wave elastography (SWE) samples. In the third step, SVM and SoftMax functions are used to classify liver fibrosis. A five-class model (normal, F1, F2, F3, and F4) was developed. The result illustrates how successfully the CNN-SoftMax and CNN-SVM classifiers classified liver fibrosis in the test dataset, with 97.18% and 98.59% accuracy, respectively.

*This is an open access article under the [CC BY-SA](#) license.*



## Corresponding Author:

Zainab Sattar Jabbar

Department of Biomedical Engineering, College of Engineering, Al-Nahrain University

Al Jadriyah Bridge, Baghdad, Iraq

Email: st.zainab.s.jabbar@ced.nahrainuniv.edu.iq

## 1. INTRODUCTION

Liver fibrosis develops as a result of structural or functional changes in the liver induced by viruses, immunological responses, and toxic assaults [1], [2]. The severity of liver fibrosis is linked to the risk of developing cirrhosis and cirrhosis-related complications [3]. The standard method for assessing liver fibrosis is currently a liver biopsy. However, it does have some drawbacks. It is an invasive procedure, with severe complications occurring in up to 1% of biopsy cases [4], [5]. Because biopsies only make up a small fraction of the overall liver, there is bound to be some sampling error [6].

As a result, noninvasive methods for detecting liver fibrosis, such as transient elastography, shear wave elastography, and magnetic resonance elastography, are becoming more popular [7]–[9]. The use of ultrasound shear wave elastography to identify advanced liver fibrosis has shown benefits as a non-invasive and low-cost approach. Ultrasound is used to create and measure tissue shear waves, which are then utilized to determine tissue stiffness. To determine tissue stiffness and fibrosis staging, a technician must manually select tissue for shear wave elastography (SWE) excitation using ultrasound imaging guidance, then measure tissue stiffness over a manually specified field of interest (ROI) within the stimulated tissue and also average tissue

stiffness from several sources (3–10) independently acquired images. The current process's manual nature increases inter-operator variability and output quality, with blood arteries, bile ducts, and the liver capsule frequently being included in the ROI by mistake, resulting in unusually high shear wave speeds for the beneath liver parenchyma [10].

Lee *et al.* [11] in 2020, developed a four model (F0 vs. F1 vs. F23 vs. F4). A total of 13,608 ultrasonography images from 3446 patients were used to train a diffusion-convolutional neural networks (DCNN). The accuracy of the four-class model was 76.4%. Dandan *et al.* [12] in 2019 proposed a strategy for classifying diffuse liver disorders based on multimodal aspects in ultrasound images. The convolutional neural network (CNN) was used to extract image structure characteristics, and the multi-scale gray-level co-occurrence matrix (MGLCM) and wavelet multi-sub-bands co-occurrence matrix (WMCOM) were used to extract image texture features WMCM. These two types of characteristics were combined to form multimodal features, which were then fed into a light gradient boosting machine (GBM) classifier as input. The proposed method was used to classify 2942 liver ultrasound images. Normal, fatty liver disease, and liver fibrosis classification accuracies are 82.1%, 85.0%, and 80.9%, respectively. Gatos *et al.* [13] in 2017 proposed a computer aided diagnosis system that uses to classify chronic liver disease from ultrasound shear wave elastography images. To quantify 85 pictures, the suggested algorithm uses an inverse mapping technique. The support vector machines (SVM) model had the highest classification accuracy of 87.0%. Deep learning technology was used to diagnose cirrhosis by Liu *et al.* [14]. CNN was used by Liu *et al.* [14] in 2017 in their study to create characteristics from ultrasound pictures. Liu *et al.* [14] used SVM as a classifier to discriminate between normal and abnormal livers, and the proposed method's accuracy was 96%. Kagadis *et al.* [15] in 2020 compared certain popular deep learning pre-trained networks with and without augmentation, using temporally stable and complete elastograms, and proposed acceptable deep learning strategies for chronic liver disease diagnosis and progression assessment. A total of 200 chronic liver disease patients with a verified liver biopsy were evaluated using the conventional ultrasound (US)/SWE method. Four pictures of the same part of the liver were saved and analyzed in order to obtain elastograms and rule out temporally unstable areas. Googlnet, Alexnet, Vgg16, Resnet50, and Densenet201, with and without augmentation, were fed complete and temporally stable masked elastograms for each patient. The networks were tested for recognizing chronic liver disease stages in seven classification schemes over 30 repetitions. The highest mean accuracies were found in all networks, ranging from 87.2 % to 97.4 %. Table 1 shows a comparison of existing deep learning-based liver fibrosis diagnosis approaches with the performance of the proposed system on various imaging datasets. It should be noted that the proposed system outperformed the other existing systems in terms of performance.

Table 1. Other methods are compared to the proposed method

Study	Method	Imaging	Accuracy %
Lee <i>et al.</i> [11]	DNN	US	76%
Dandan <i>et al.</i> [12]	CNN	US	80.9%
Gatos <i>et al.</i> [13]	SVM	US SWE	87.0
Gatos <i>et al.</i> [16]	CNN	US SWE	95%
Liu <i>et al.</i> [14]	SVM	US SWE	96%
Kagadis <i>et al.</i> [15]	Resnet50	US SWE	97.4%
Our model	CNN-SVM	US SWE	98.59

The purpose of this paper was to use (US-SWE) images from healthy patients and patients with liver fibrosis to train a CNN algorithm to distinguish between healthy and fibrotic livers and classify the stages of fibrosis (multi-classification). The main contribution of the proposed system is the following: The proposed system focused on creating a machine learning-based hybrid model (CNN-SVM) to diagnose liver fibrosis in SWE images, adopting fewer parameters than the most modern deep learning models SVM, the proposed method is highly accurate, employing (CNN-SoftMax) or (CNN-SVM), which alleviates the difficulties associated with handling more fibrosis cases.

## 2. METHOD

### 2.1. Dataset gathering

We have collected our data from a LOGIQ E9 ultrasound shear wave elastography imaging machine. The dataset consists of 700 US/SWE images (150 normal liver SWE images and F=150, F2=150, F3=114, F4=136). The datasets are split into two samples: for the training phase (90%) and the testing phase (10%). In order to establish a fixed size for all images in the dataset to be appropriate for further processing, the SWE images are scaled to a size of (256×256) pixels.

## 2.2. Dataset preparation

We categorized our data before preprocessing. We've labeled the dataset as multistage because we're employing multi-classification (normal, F1, F2, F3, and F4). Normal tissue is healthy (i.e., there is no fibrosis), whereas other stages are fibrosis tissue. Stages F1 and F2 are mild fibrosis; stage F3 is moderate fibrosis, and stage F4 is severe fibrosis (cirrhosis). The images collected from the US/SWE were in digital imaging and communications in medicine (DICOM) format. The DICOM images contained metadata containing patient information. As a result, all metadata is lost when images are converted into bitmap format. Furthermore, because computer vision processing algorithms deal with images as raw pixel values, it's easier to convert images to the (.bmp) format before using them as input to the CNN model to save computational power.

## 2.3. Data pre-processing

Our data pre-processing consists of many parts shown in Figure 1. First step is Image cropping to a large texture ROI that only contains liver pixels as shown in Figure 2. To crop the images, we utilized the (finding extreme point in contour) technique using opencv in Python. Second, the images are three-channel colorful images red, green, and blue (RGB), so they are converted to grayscale images in order to reduce processing time (one channel). Third step is image enhancement. SWE image preprocessing is performed using the contrast limited adaptive histogram equalization (CLAHE) approach in this step. CLAHE is a contrast enhancement approach that efficiently improves image contrast, reduces noise and blurring, sharpens features, and displays image details like as edge detection without affecting the SWE image's inherent structure. Forth step is image resizing. The time it takes to train a neural network model is cut in half when images are resized. Using python and opencv, we resized the images. Finally, normalization: To speed up the processing, divide the image elements by 255 to create the values between 0 and 1.

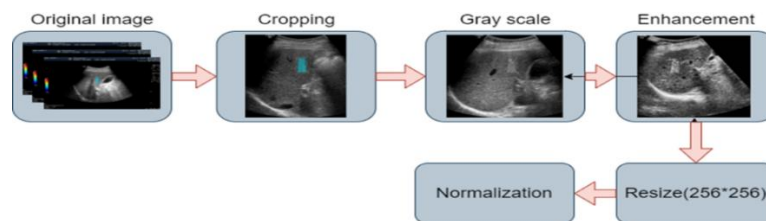


Figure 1. The pre-processing steps

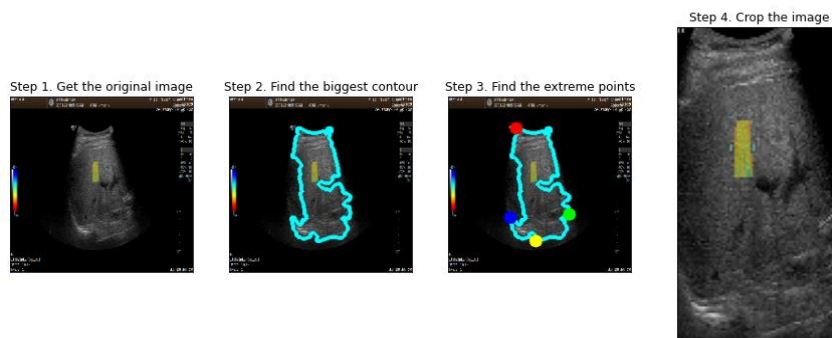


Figure 2. Pre-processing process (cropping by contour detection algorithm)

## 2.4. Proposed model

The design of the CNN architecture illustrated in Figure 3. To detect and analyze available features in SWE images, a CNN with several convolution layers and a MaxPooling layer was used in this study. The following is the structure of the feature extraction:

- The input layer is the first layer that contain the image of ultrasound (SWE image).
- The convolutional layer: Conv2D was used in our proposed CNN model. In our model, we employed five conv2D layers.
- The pooling layer: MaxPooling2D was utilized in this model. We utilized a MaxPool2D layer for each

Conv2D layer. As a result, we used five MaxPool2D layers.

- The flatten layer: we used a flatten layer after using the pooling layer to flat the network system in our model.
- The dense layer: we utilized dense layers after the flatten layer.
- The activation function: we used the SoftMax function from (1) with the other dense layer and the rectified linear unit (ReLU) function from (2) [17].

$$\sigma(\vec{z}) = \frac{e^{z_i}}{\sum_{j=1}^k e^{z_j}} \tag{1}$$

$$\text{ReLU} = \max(0, x) \tag{2}$$

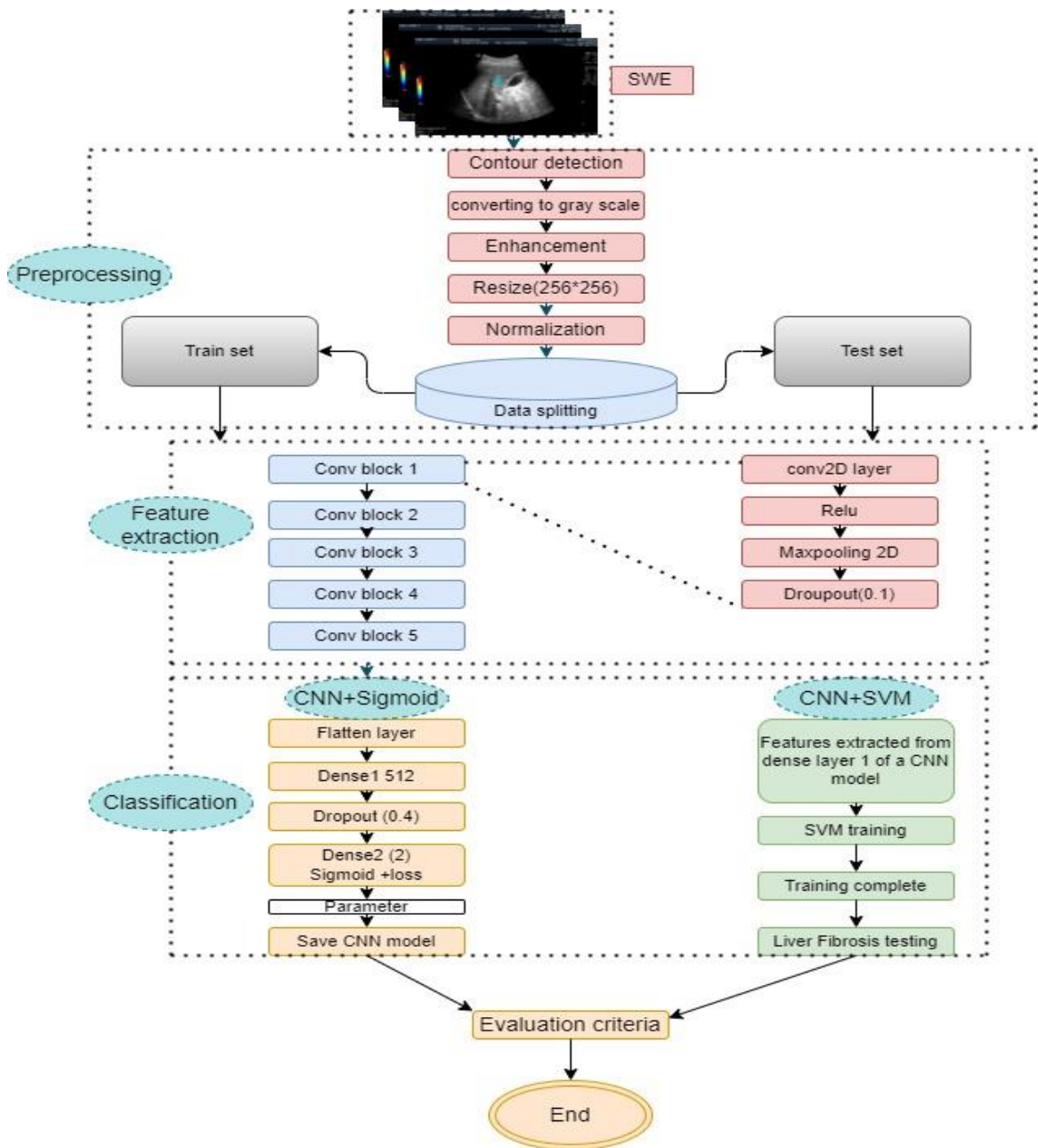


Figure 3. Block diagram of the proposed system

The weights were modified with a categorical cross-entropy loss function and the optimizer is Adam with a learning rate of (0.001). The proposed model is summarized in Table 2. ReLU is an activation function for each convolutional layer. The pooling layer is a technique for down sampling a collection of nearby pixels into a single pixel. This down sampling reduced the size of the activation maps image from 4×4 to 2×2. Overfitting can be solved by pooling layers, and MaxPool has proven to be the most effective [18].

Table 2 Exhibit the summary of CNN model

No.	Layer name	Input layer	Output layer	Filter size	Parameter
1	Convolution 1 & ReLU	(256, 256, 1)	(256, 256, 20)	(3×3), 1	560
2	MaxPooling1 & Dropout (0.1)	(256, 256, 20)	(128, 128, 20)	(2×2), 2	0
3	Convolution 2 & ReLU	(128, 128, 20)	(128, 128, 40)	(3×3), 1	7240
4	MaxPooling2 & Dropout (0.1)	(128, 128, 40)	(64, 64, 40)	(2×2), 2	0
5	Convolution 3 & ReLU	(64, 64, 40)	(64, 64, 80)	(3×3), 1	28880
6	MaxPooling3 & Dropout (0.1)	(64, 64, 80)	(32, 32, 80)	(2×2), 2	0
7	Convolution 4 & ReLU	(32, 32, 80)	(32, 32, 160)	(3×3), 1	115360
8	MaxPooling4 & Dropout (0.1)	(32, 32, 16+0)	(16, 16, 160)	(2×2), 2	0
9	Convolution 5 & ReLU	(16, 16, 160)	(16, 16, 320)	(3×3), 1	461120
10	MaxPooling5 & Dropout (0.1)	(16, 16, 320)	(8, 8, 320)	(2×2), 2	0
11	Fully connected layer (Flatten)	(8, 8, 320)	20480	/	0
12	Dense layer 1 (512)	20480	512	/	10486272
13	Dropout layer (0.4)	/	/	/	0
14	Dense layer 2 (5) SoftMax	512	5	/	2565
					11,101,637

## 2.5. Classification phase

Features of SWE images are used to appropriately categorize patients whether they are infected or not for the diagnosis of liver fibrosis infected cases. Classification is utilized to introduce diagnosis prediction (normal, fibrosis stages (F1, F2, F3, F4)) based on the extracted attribute. This research employs two classifiers (SoftMax and SVM).

### 2.5.1. SoftMax classifier

After the flatten layer, the dense architecture has one fully connected layer with an activation function (ReLU). The activation function for the dropout layer with a ratio of (0.4) and the dense layer for classification was SoftMax. Since SoftMax values are in between 0 and 1, and if all of the features are performed using the formula as (3), the result is 1.

$$\text{softmax}(xi) = \frac{\exp(xi)}{\sum_{j=0}^n \exp(xj)} \quad (3)$$

$X_i$  is the production associated with class  $I$ , where  $j$  is the number of classes. The SoftMax function is extensively used to estimate probabilities and conduct multi-classifications [19].

### 2.5.2. Support vector machine classifier

SVM is the second classification method. To provide results for identifying SWE images, the SVM classifier was added to the retrieved feature of the fully connected layer of CNN. The standardization of the feature values obtained (feature vector) from CNN, which speeds up processing because these characteristics will be within a specified range after standardization. SWE image classification is split into two stages. Using the trained CNN model, the features of the input data are automatically extracted during the SVM's training phase. To complete SVM training, the retrieved representative feature data and their related labels are fed into the model [20].

## 2.6. Proposed model's performance

Precision, recall, f1 score, and accuracy were used to assess the performance of our suggested model. The following are the accuracy, f1-score, and precision equations:

$$\text{Accuracy equation [21]–[24]} = TP + \frac{TN}{TP} + TN + P + N \quad (4)$$

$$\text{Sensitivity equation [21]–[23]} = TP + TN/TP + N \quad (5)$$

$$\text{Precision equation [21]–[23]} = TP + TN/TP + P \quad (6)$$

$$F1\text{-score equation [21]–[23], [25]} = (Precision \times Sensitivity) / (Precision + Sensitivity) \quad (7)$$

where: TP=correct positive, TN=true negative, P=positive condition, N=negative condition.

Figure 4 displays the proposed model's main categorization criteria. The following are the parameters of the given model and test SWE images: true positive is a correct classification of a positive prognosis, such as normal diagnosed as normal, false positive is an incorrect classification of a positive diagnosis, such as fibrosis liver diagnosed as normal, true negative is a correct classification of a negative diagnosis, such as fibrosis liver diagnosed as fibrosis liver, and false negative is an incorrect classification of a negative diagnosis, such as normal diagnosed as fibrosis liver.

### 3. RESULTS AND DISCUSSION

#### 3.1. Requirements for software and hardware

The proposed liver fibrosis classification system is based on a Lenovo personal computer with specifications that include NVidia GTX 1650 4GB, AMD Ryzen5 5600H CPU, 512GB SSD storage, and 16GB RAM. TensorFlow open-source framework (a Google open-source programming library that is concentrated on supporting tensors to produce successful work), Keras (a neural network library based on TensorFlow written in Python, and also open-source), and Python (Python version 3.9.7, Jupyter notebook) are used for the implementation of the CNN code. The system relied on open source libraries such as Open, Scikit Learn, and Pandas. These libraries are dedicated to dealing with machine learning and data analysis.

#### 3.2. Results of the features extraction steps

The feature extraction steps are carried out using CNN, which is made up of five successful convolutional blocks, each of which has four layers: a convolutional layer with a rectified linear unit (ReLU) activation function, a MaxPooling layer, and a dropout layer. The CNN model's convolution layer extracts features or manifestations of SWE images by passing many different filters over a SWE image, such as edge detection, vertical, horizontal, and diagonal lines, curves, corners, color contrast sensitive filters, and so on. Each of these filters generates a feature map, which shows the spatial patterns where the feature is located. The feature map is then passed through a non-linear activation function ReLU. Each filter has a size of (3,3), and the number of filters in each layer is (20, 40, 80, 160, 320). The MaxPooling layer reduces computational power by reducing the dimensions of features maps to half because the kernel size is equal to (2, 2). This contributes to reducing the over-fitting problem.

#### 3.3. Result of shear wave elastography image classification using SoftMax function

The extracted features are passed to the layers for classification after the feature extraction stage. The confusion matrix of features extracted by CNN is shown in Figure 4. The confusion matrix of the test sample yielded the highest accuracy of 97.18%, sensitivity of 97.2%, precision of 97.2%, and an F1 score of 97.4%. To highlight the high outcomes of our suggested model, as shown Figure (5) we plotted model accuracy in Figure 5(a) and model loss in Figure 5(b). As illustrated in these graphs, our proposed CNN model is neither under-fit nor over-fit. This explains why, in terms of precision, recall, and f1-score, we surpassed the competition.

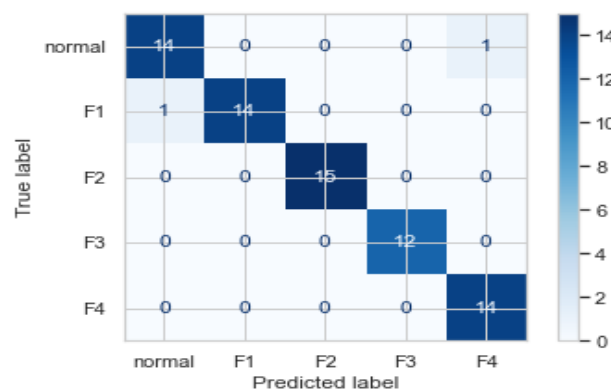
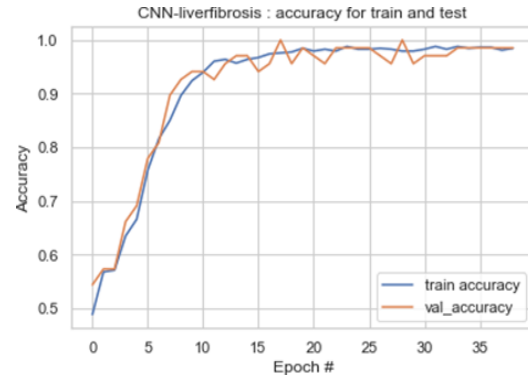
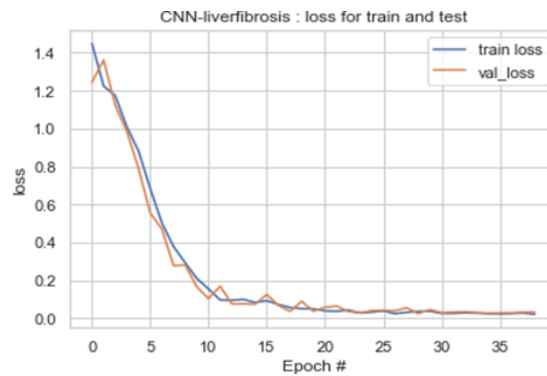


Figure 4. Confusion matrix of the test sample for SoftMax classifier



(a)



(b)

Figure 5. To highlight the high outcomes of our suggested model; (a) model accuracy graph and (b) model loss graph

**3.4. Result of shear wave elastography image classification using support vector machine**

The features from the dense layer 1 of the CNN will be classified using "linear" as the kernel function in the support vector machine. The accuracy of the SVM classifier is 98.59%. The confusion matrix using the SVM classifier when the model is trained on a dataset. The confusion matrix of the test sample for the SVM classifier is shown in Figure 6.

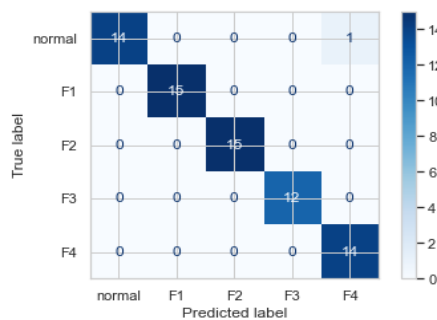


Figure 6. Confusion matrix of the test sample for SVM classifier

**3.5. Comparison results between CNN-SoftMax and CNN-SVM**

Table 3 compares the results of performance measures using CNN-SoftMax to the results of performance measures using CNN-SVM, showing that CNN-SVM outperformed CNN- SoftMax. CNN have convolutional layers, which contain important filters for extracting features from the SWE image and have thus been used to extract features. The SVM is built on the principle of finding the optimal hyper plane for separating a data set into two groups in an efficient way. To maximize the results of the margin (the distance between the

hyper plane and the closest point of any of the data sets), the SVM provides the ability of generalization better compared to using SoftMax function as a classifier.

Table 3. Comparison results between CNN-SoftMax and CNN-SVM

Method	Sensitivity	Precision	F1_score	Accuracy
CNN-SoftMax	97.2	97.2	97.4	97.18
CNN-SVM	98.6	98.6	98.8	98.5

#### 4. CONCLUSION

The proposed system addresses the issue of detecting liver fibrosis in US/SWE liver images. The preprocessing phase is essential for working efficiently with CNN and producing higher-quality results. On SWE images, the proposed method was evaluated using the CNN-SoftMax function and CNN-SVM classifiers; accuracy was 98.5% with CNN-SVM and 97.18% with CNN-SoftMax, respectively. This study compared the CNN-SoftMax and CNN-SVM algorithms, and the experimental results show that the CNN-SVM algorithm performs better than the CNN-SoftMax algorithm. The proposed method, which employs CNN-Softmax or CNN-SVM, is highly accurate, reducing the problems associated with dealing with more liver fibrosis. The model achieved higher accuracy with fewer parameters (11,101,637) and less computational power. VGG16 is trained and tested using the same dataset. Additionally, the proposed system outperformed it. Finally, in future work, we will expand the capabilities of the proposed system by using a large dataset of US/SWE images (thousands of images).

#### REFERENCES

- [1] "Global, regional, and national age–sex specific all-cause and cause-specific mortality for 240 causes of death, 1990–2013: a systematic analysis for the Global Burden of Disease Study 2013," *The Lancet*, vol. 385, no. 9963, pp. 117–171, Jan. 2015, doi: 10.1016/S0140-6736(14)61682-2.
- [2] D. S. Manning and N. H. Afdhal, "Diagnosis and quantitation of fibrosis," *Gastroenterology*, vol. 134, no. 6, pp. 1670–1681, May 2008, doi: 10.1053/j.gastro.2008.03.001.
- [3] J. Vergniol *et al.*, "Noninvasive tests for fibrosis and liver stiffness predict 5-year outcomes of patients with chronic hepatitis C," *Gastroenterology*, vol. 140, no. 7, pp. 1970–1979.e3, Jun. 2011, doi: 10.1053/j.gastro.2011.02.058.
- [4] L. B. Seeff *et al.*, "Complication rate of percutaneous liver biopsies among persons with advanced chronic liver disease in the HALT-C trial," *Clinical Gastroenterology and Hepatology*, vol. 8, no. 10, pp. 877–883, Oct. 2010, doi: 10.1016/j.cgh.2010.03.025.
- [5] B. R. Stotland and G. R. Lichtenstein, "Liver biopsy complications and routine ultrasound," *The American journal of gastroenterology*, vol. 91, no. 7, pp. 1295–6, Jul. 1996, [Online]. Available: <http://www.ncbi.nlm.nih.gov/pubmed/8677980>.
- [6] M. Guido and M. Rugge, "Liver biopsy sampling in chronic viral hepatitis," *Seminars in Liver Disease*, vol. 24, no. 1, pp. 89–97, Jan. 2004, doi: 10.1055/s-2004-823103.
- [7] "EASL-ALEH clinical practice guidelines: non-invasive tests for evaluation of liver disease severity and prognosis," *Journal of Hepatology*, vol. 63, no. 1, pp. 237–264, Jul. 2015, doi: 10.1016/j.jhep.2015.04.006.
- [8] M. Giuffrè *et al.*, "Alanine aminotransferase and spleno-portal dynamics affect spleen stiffness measured by point shear-wave elastography in patients with chronic hepatitis C in the absence of significant liver fibrosis," *Journal of Ultrasound*, vol. 24, no. 1, pp. 67–73, Mar. 2021, doi: 10.1007/s40477-020-00456-9.
- [9] F. Ravaioli, M. Montagnani, A. Lisotti, D. Festi, G. Mazzella, and F. Azzaroli, "Noninvasive assessment of portal hypertension in advanced chronic liver disease: an update," *Gastroenterology Research and Practice*, vol. 2018, pp. 1–11, Jun. 2018, doi: 10.1155/2018/4202091.
- [10] G. Ferraioli *et al.*, "Liver ultrasound elastography: an update to the world federation for ultrasound in medicine and biology guidelines and recommendations," *Ultrasound in Medicine & Biology*, vol. 44, no. 12, pp. 2419–2440, Dec. 2018, doi: 10.1016/j.ultrasmedbio.2018.07.008.
- [11] J. H. Lee *et al.*, "Deep learning with ultrasonography: automated classification of liver fibrosis using a deep convolutional neural network," *European Radiology*, vol. 30, no. 2, pp. 1264–1273, Feb. 2020, doi: 10.1007/s00330-019-06407-1.
- [12] L. Dandan, M. Huanhuan, L. Xiang, J. Yu, J. Jing, and S. Yi, "Classification of diffuse liver diseases based on ultrasound images with multimodal features," in *2019 IEEE International Instrumentation and Measurement Technology Conference (I2MTC)*, May 2019, pp. 1–5, doi: 10.1109/I2MTC.2019.8827174.
- [13] I. Gatos *et al.*, "A machine-learning algorithm toward color analysis for chronic liver disease classification, employing ultrasound shear wave elastography," *Ultrasound in Medicine & Biology*, vol. 43, no. 9, pp. 1797–1810, Sep. 2017, doi: 10.1016/j.ultrasmedbio.2017.05.002.
- [14] X. Liu, J. Song, S. Wang, J. Zhao, and Y. Chen, "Learning to diagnose cirrhosis with liver capsule guided ultrasound image classification," *Sensors*, vol. 17, no. 12, p. 149, Jan. 2017, doi: 10.3390/s17010149.
- [15] G. C. Kagadis *et al.*, "Deep learning networks on chronic liver disease assessment with fine-tuning of shear wave elastography image sequences," *Physics in Medicine & Biology*, vol. 65, no. 21, p. 215027, Nov. 2020, doi: 10.1088/1361-6560/abae06.
- [16] I. Gatos *et al.*, "Temporal stability assessment in shear wave elasticity images validated by deep learning neural network for chronic liver disease fibrosis stage assessment," *Medical Physics*, vol. 46, no. 5, pp. 2298–2309, May 2019, doi: 10.1002/mp.13521.
- [17] S. Sharma, S. Sharma, and A. Athaiya, "Activation functions in neural networks," *International Journal of Engineering Applied Sciences and Technology*, vol. 04, no. 12, pp. 310–316, May 2020, doi: 10.33564/IJEAST.2020.v04i12.054.
- [18] Gong *et al.*, "A novel deep learning method for intelligent fault diagnosis of rotating machinery based on improved CNN-SVM and multichannel data fusion," *Sensors*, vol. 19, no. 7, p. 1693, Apr. 2019, doi: 10.3390/s19071693.
- [19] L. Taylor and G. Nitschke, "Improving deep learning with generic data augmentation," in *2018 IEEE Symposium Series on Computational Intelligence (SSCI)*, Nov. 2018, pp. 1542–1547, doi: 10.1109/SSCI.2018.8628742.






- [20] K. S. Nugroho, A. Y. Sukmadewa, A. Vidiyanto, and W. F. Mahmudy, "Effective predictive modelling for coronary artery diseases using support vector machine," *IAES International Journal of Artificial Intelligence (IJ-AI)*, vol. 11, no. 1, pp. 345–355, Mar. 2022, doi: 10.11591/ijai.v11.i1.pp345-355.
- [21] C. Nicholson, "Evaluation metrics for machine learning—accuracy, precision, recall, and F1 defined." [wiki.pathmind.com/https://wiki.pathmind.com/accuracy-precision-recall-f1](https://wiki.pathmind.com/accuracy-precision-recall-f1) (accessed Oct. 1, 2022).
- [22] M. A. Rahman, "Automatic selection of high quality initial seeds for generating high quality clusters without requiring any user inputs," Ph.D dissertation, Charles Sturt University, Australia, 2014.
- [23] M. A. Rahman, K. L.-M. Ang, and K. P. Seng, "Unique neighborhood set parameter independent density-based clustering with outlier detection," *IEEE Access*, vol. 6, pp. 44707–44717, 2018, doi: 10.1109/ACCESS.2018.2857834.
- [24] T. A. Assegie, R. Subhashni, N. K. Kumar, J. P. Manivannan, P. Duraisamy, and M. F. Engidaye, "Random forest and support vector machine based hybrid liver disease detection," *Bulletin of Electrical Engineering and Informatics*, vol. 11, no. 3, pp. 1650–1656, Jun. 2022, doi: 10.11591/eei.v11i3.3787.
- [25] I. Sadgali, N. Sael, and F. Benabbou, "Human behavior scoring in credit card fraud detection," *IAES International Journal of Artificial Intelligence (IJ-AI)*, vol. 10, no. 3, pp. 698–706, Sep. 2021, doi: 10.11591/ijai.v10.i3.pp698-706.

## BIOGRAPHIES OF AUTHORS



**Eng. Zainab Sattar Jabbar**    received the B.Sc. degree from Al-Nahrain University, College of Engineering, Biomedical Engineering Department in Iraq, 2015. Her research interests include Artificial Intelligence, Machine Learning, and Image Processing. She can be contacted at email: [st.zainab.s.jabbar@ced.nahrainuniv.edu.iq](mailto:st.zainab.s.jabbar@ced.nahrainuniv.edu.iq).






**Assist. Prof. Dr. Auns Qusai Al-Neami**    in Al-Nahrain University/College of Engineering/Biomedical Engineering Department. B.Sc. in the electrical engineering. M.Sc. in the electrical engineering. Ph.D. In the electrical engineering. Teaching in the following subjects: measurement systems, AI and expert system, computer programming, biomedical imaging analysis, bioinstrumentation systems, biomedical sensors, artificial neural network, machine learning clinical engineering, artificial organs systems, mathematics, and deep learning, advanced replaced organs, tissue engineering, advanced Infrared imaging. She can be contacted at email: [unsalneami2@gmail.com](mailto:unsalneami2@gmail.com).



**Assist. Prof. Dr. Ahmed A. Khawwam**    graduated from Kufa University College of Medicine 2013. Arab board of radiology and medical imaging 2021. European diploma in radiology 2021. Member of teaching staff in Kufa University. He can be contacted at email: [dr.ahmedkhawwam@gmail.com](mailto:dr.ahmedkhawwam@gmail.com).



**Assist. Prof. Sufian Munther Salih**    Ph.D. degree planning and regional Science, Planning and regional Science center, University of Baghdad, 2014. The main theme addressed was "Application of Healthy Cities Project features and features (Applied statistical study)", Baghdad-Iraq. MA. Degree in Planning and regional Science, Planning and regional Science center, University of Baghdad, 2005, Baghdad-Iraq. High Diploma in Applied Calculators/Information Technology College/Graduate Institute of Computer and Informatics studies/University of Information Technology now, Baghdad/1999. BA. Degree in Statistics and Informatics, College of Administration and Economy, Al Mustansiriyah University, 1997, Baghdad-Iraq. He can be contacted at email: [dr.sufian2006@gmail.com](mailto:dr.sufian2006@gmail.com).